



Segmental alterations of the corpus callosum in motor neuron disease: A DTI and texture analysis in 575 patients

Maximilian Münch^{a,1}, Hans-Peter Müller^{a,1}, Anna Behler^a, Albert C. Ludolph^{a,b}, Jan Kassubek^{a,b,*}

^a Department of Neurology, University of Ulm, Germany

^b German Center for Neurodegenerative Diseases (DZNE), Ulm, Germany

ARTICLE INFO

Keywords:

Amyotrophic lateral sclerosis
Diffusion-weighted imaging
Magnetic resonance imaging
Motor neuron disease
Neurodegenerative disease
Support vector machine

ABSTRACT

Introduction: Within the core neuroimaging signature of amyotrophic lateral sclerosis (ALS), the corpus callosum (CC) is increasingly recognized as a consistent feature. The aim of this study was to investigate the sensitivity and specificity of the microstructural segmental CC morphology, assessed by diffusion tensor imaging (DTI) and high-resolution T1-weighted (T1w) imaging, in a large cohort of ALS patients including different clinical phenotypes. **Methods:** In a single-centre study, 575 patients with ALS (classical phenotype, N = 432; restricted phenotypes primary lateral sclerosis (PLS) N = 55, flail arm syndrome (FAS) N = 45, progressive bulbar palsy (PBP) N = 22, lower motor neuron disease (LMND) N = 21) and 112 healthy controls underwent multiparametric MRI, i.e. volume-rendering T1w scans and DTI. Tract-based fractional anisotropy statistics (TFAS) was applied to callosal tracts of CC areas I-V, identified from DTI data (tract-of-interest (TOI) analysis), and texture analysis was applied to T1w data. In order to further specify the callosal alterations, a support vector machine (SVM) algorithm was used to discriminate between motor neuron disease patients and controls.

Results: The analysis of white matter integrity revealed predominantly FA reductions for tracts of the callosal areas I, II, and III (with highest reductions in callosal area III) for all ALS patients and separately for each phenotype when compared to controls; texture analysis demonstrated significant alterations of the parameters entropy and homogeneity for ALS patients and all phenotypes for the CC areas I, II, and III (with again highest reductions in callosal area III) compared to controls. With SVM applied on multiparametric callosal parameters of area III, a separation of all ALS patients including phenotypes from controls with 72% sensitivity and 73% specificity was achieved. These results for callosal area III parameters could be improved by an SVM of six multiparametric callosal parameters of areas I, II, and III, achieving a separation of all ALS patients including phenotypes from controls with 84% sensitivity and 85% specificity.

Discussion: The multiparametric MRI texture and DTI analysis demonstrated substantial alterations of the frontal and central CC with most significant alterations in callosal area III (motor segment) in ALS and separately in all investigated phenotypes (PLS, FAS, PBP, LMND) in comparison to controls, while no significant differences were observed between ALS and its phenotypes. The combination of the texture and the DTI parameters in an unbiased SVM-based approach might contribute as a **neuroimaging marker** for the assessment of the CC in ALS, including subtypes.

1. Introduction

Amyotrophic lateral sclerosis (ALS) is a neurodegenerative motor neuron disease (MND) which is characterized by the degeneration of upper and lower motor neurons (UMN, LMN) and is regarded as a multi-system disorder with extra-motor involvement as a part of the disease

process (van Es et al., 2017; Swinnen and Robberecht, 2014). The concept of the restricted phenotypes in the revisions of the El Escorial criteria (Ludolph et al., 2015) includes primary lateral sclerosis (PLS) with predominant UMN involvement, flail arm syndrome (FAS), progressive bulbar palsy (PBP), and progressive muscular atrophy (PMA)/lower motor neuron disease (LMND) with pure LMN degeneration

* Corresponding author at: Dept. of Neurology, University of Ulm, Oberer Eselsberg 45, 89081 Ulm, Germany.

E-mail address: jan.kassubek@uni-ulm.de (J. Kassubek).

¹ shared first authorship.

<https://doi.org/10.1016/j.nicl.2022.103061>

Received 26 March 2022; Received in revised form 15 May 2022; Accepted 26 May 2022

Available online 28 May 2022

2213-1582/© 2022 The Author(s). Published by Elsevier Inc. This is an open access article under the CC BY-NC-ND license (<http://creativecommons.org/licenses/by-nc-nd/4.0/>).

(Ludolph et al., 2015), a concept which is currently discussed (de Vries et al., 2019; Finegan et al., 2019).

The potential of multiparametric magnetic resonance imaging (MRI) in ALS from a clinico-diagnostic and from an academic perspective is widely recognised (Chiò et al., 2014; Filippi et al., 2015), and the core neuroimaging signature of ALS includes motor cortex, corticospinal tract, brainstem, and spinal cord degeneration, with subcortical grey matter degeneration also being observed (Kassubek and Müller, 2020; Agosta et al., 2018; Bede et al., 2018). As a consistent structure in ALS-associated regional WM degeneration, the corpus callosum (CC) is increasingly recognized e.g. by decreased fractional anisotropy (FA) and increased mean diffusivity (Foerster et al., 2013; Turner and Verstraete, 2015) and may reflect bilateral cortical involvement or interhemispheric spread of pathology (Filippini et al., 2010). Thus, CC degeneration in association with ALS has been highlighted by post mortem studies (Cardenas et al., 2017) and was repeatedly demonstrated *in vivo* by computational neuroimaging as part of the widespread white matter changes in ALS (Agosta et al., 2010; Kassubek et al., 2012; Agosta et al., 2014; Müller et al., 2016; Kassubek et al., 2018; Tu et al., 2020; Bede et al., 2020), including a multicenter study pooling DTI data of ALS patients from eight sites (Müller et al., 2016). The decrease in CC white matter integrity in patients with MND has been localized to motor-related areas (Chapman et al., 2014), corresponding to segment III according to the fibre tractography-based scheme proposed by Hofer and Frahm which subdivides the CC into five different areas I to V (Hofer and Frahm, 2006). Such a focal degeneration of the motor area III could be demonstrated by multiparametric T1-weighted MRI/DTI-based analysis in sporadic ALS (Müller et al., 2020) and specifically in familial ALS with *C9orf72* expansion (Müller et al., 2021). In line with these results, an application of a machine learning (ML) algorithm to MRI data of ALS patients with respect to the linear coefficients demonstrated that the CC texture homogeneity contributed the most to accurate classification, followed by the corticospinal tract (CST) FA and CC FA (Kocar et al., 2021).

The current study was designed to analyse the sensitivity and specificity of multiparametric MRI in evaluating the segmental MRI signature of the CC in ALS including different clinical phenotypes ('classical' ALS, PLS, FAS, PBP, and LMND). The tract-based analysis of DTI data and T1 MRI-based texture analysis were applied to the five different CC areas in order to investigate *in vivo* the ALS-associated callosal alteration pattern and how to automatically investigate CC morphology in ALS by an SVM-based approach.

2. Methods

2.1. Subjects

Five hundred and seventy-five patients with ALS or its variants (restricted phenotypes PLS N = 55, FAS N = 45, PBP N = 22, LMND N = 21) and 112 healthy controls underwent multiparametric MRI, i.e., volume-rendering T1-weighted scans and DTI. All patients and controls gave written informed consent for the study protocol according to institutional guidelines which had been approved by the Ethics

Table 1

Characteristics of patients and healthy controls. ALS – amyotrophic lateral sclerosis; PLS – primary lateral sclerosis; LMND – lower motor neuron disease; PBP – progressive bulbar palsy; FAS – flail arm syndrome; ALS-FRS-R – revised ALS functional rating scale; *t-test: all MND vs controls; **Kruskal-Wallis-test: six groups (five MND groups and control group).

	controls	all MND	p (t-test*)	ALS	PLS	FAS	PBP	LMND	p (Kruskal-Wallis**)
no. of subjects	112	575	–	432	55	45	22	21	–
male/female	56/56	339/236	0.08	256/176	24/31	32/13	9/13	18/3	0.001
age / years	62 ± 10	63 ± 11	0.2	63 ± 12	61 ± 10	64 ± 11	70 ± 11	64 ± 11	0.01
ALS-FRS-R	–	39 ± 10	–	39 ± 7	37 ± 9	41 ± 6	43 ± 3	42 ± 7	0.008
decrease of ALS-FRS-R per year	–	6.0 ± 5.7	–	–6.4 ± 5.9	–3.1 ± 4.4	–5.2 ± 4.9	–7.5 ± 8.9	–5.1 ± 2.9	< 0.001
disease duration / years	–	1.8 ± 2.0	–	1.4 ± 1.4	5.2 ± 4.3	1.7 ± 1.3	0.8 ± 0.4	1.2 ± 1.0	< 0.001

Committee of Ulm University, Germany (reference No. 327/21).

2.1.1. Patient characteristics

Patients had to meet the following criteria: no family history of MND, no clinical diagnosis of frontotemporal dementia (FTD), no mutations of major genes related to hereditary spastic paraparesis if investigated, no other major systemic, psychiatric or neurological illnesses, no history of substance abuse. Routine MRI scans were used to exclude any brain or cervical cord abnormalities suggesting a different etiology of the clinical symptoms. All patients underwent standardized clinical, neurological, and routine laboratory examinations. A summary of the patients' characteristics is given in Table 1.

2.1.1.1. 'Classical' amyotrophic lateral sclerosis. A group of 432 patients with sporadic ALS were included (256 males, age 63 ± 12 years). All patients had a diagnosis of definitive or probable ALS made according to the El Escorial diagnostic criteria (Brooks et al., 2000; Ludolph et al., 2015). None of the patients had a clinical diagnosis of frontotemporal dementia (FTD). The ALS patients presented with a revised ALS functional rating scale (ALS-FRS-R) (Cedarbaum et al., 1999) of 39 ± 7; disease duration was 1.4 ± 1.4 years.

2.1.1.2. Primary lateral sclerosis. Fifty-five PLS patients (24 males, age 61 ± 19 years) were included who met the proposed diagnostic criteria for PLS (Wais et al., 2017). PLS patients presented an ALS-FRS-R of 38 ± 8; disease duration was 5.7 ± 8.3 years.

2.1.1.3. Flail arm syndrome. Forty-five FAS patients (32 males, age 64 ± 11 years) were included who met the diagnostic criteria for FAS (Wijesekera et al., 2009; Hübers et al., 2016). FAS was diagnosed in patients with pareses of both upper limbs and without bulbar and lower limbs symptoms during a time period of 12 months after their visit (Hübers et al., 2016). In this group, 42 patients presented with bilateral paresis in the arms at the date of MRI, while unilateral arm symptoms at the date of MRI were observed in 3 patients. Further follow-up after MRI was lost in 15 out of 45 patients. Four patients progressed to the bulbar region and 19 to the lumbar region, while 7 patients showed no spreading to other body regions at the time of data analysis. At the time of data analysis, 12 patients had died with a mean survival of 41 ± 12 months. FAS patients presented with an ALS-FRS-R of 41 ± 6; disease duration was 2.3 ± 3.9 years.

2.1.1.4. Progressive bulbar palsy. Twenty-two PBP patients (9 males, age 70 ± 11 years) were included who met the diagnostic criteria for PBP. All PBP patients showed an isolated bulbar onset with a progressive affection of the lower cranial nerves causing dysarthria and/or dysphagia, tongue wasting, and fasciculations over six months before they developed spinal symptoms of motor neuron disease (Chiò et al., 2011). None of the patients had any bulbar upper motor neuron signs, neither at onset nor at the time of scanning. Clinically, all patients had an isolated bulbar onset and a prominent progressive bulbar syndrome at the time of MRI scanning, but many of the patients already showed

beginning spinal symptoms with fasciculations and pareses which had started after the first six months after symptom onset, as compatible with the diagnosis PBP. PBP patients presented with an ALS-FRS-R of 43 ± 3 ; disease duration was 1.1 ± 0.7 years.

2.1.1.5. Lower motor neuron disease (LMND). Twenty-one patients (18 males, age 65 ± 10 years) presented with the diagnosis of adult LMND which was based on the presence of pure LMN findings in two or more regions (bulbar, cervical, thoracic, lumbosacral) at the first evaluation, including evidence of LMN involvement on neurological examination (weakness and muscular atrophy, absent tendon reflexes), electrophysiological evidence of LMN involvement on standardized needle electromyography, and no motor nerve conduction block. All patients showed typical pareses without central motor or oculomotor signs on clinical presentation. According to a previous study (Rosenbohm et al., 2016), the LMND cohort was limited to patients with disease duration below 4 years under the assumption of an ALS-like prognosis. It seemed safe to use a 4 year criterion in the light of a prospective population-based study of ALS in which 70% of patients with LMN signs had developed UMN and bulbar signs characteristic of ALS after six years (van den Berg-Vos et al., 2003). The age at onset was > 40 years. LMND patients presented with an ALS-FRS-R of 41 ± 7 ; disease duration was 1.4 ± 0.8 years.

2.1.2. Controls

The patients were compared to a group of 112 age-matched healthy controls. All control individuals had no family history of neuromuscular disease and had no history of neurological, psychiatric, or other major medical condition and were recruited from among spouses of patients and by word of mouth. Gross brain pathology, including vascular brain alterations, was excluded by conventional MRI including fluid-attenuated inversion recovery sequences.

2.2. MRI acquisition

DTI scanning was performed on the same 1.5 Tesla Magnetom Symphony (Siemens Medical, Erlangen, Germany) for all subjects. Three DTI study protocols were used. DTI study protocol A consisted of 13 volumes (45 slices, 128×128 pixels, slice thickness 2.2 mm, pixel size $1.5 \text{ mm} \times 1.5 \text{ mm}$) representing 12 gradient directions (GD) ($b = 800 \text{ s/mm}^2$) and one scan with gradient 0 ($b = 0$). The echo time (TE) and repetition time (TR) were 93 ms and 8000 ms, respectively. Five scans were averaged online by the scanner software in image space. DTI study protocol B consisted of 52 volumes (64 slices, 128×128 pixels, slice thickness 2.8 mm, pixel size $2.0 \text{ mm} \times 2.0 \text{ mm}$), representing 48 GD ($b = 1000 \text{ s/mm}^2$) and four scans with $b = 0$; TE and TR were 95 ms and 8000 ms. DTI study protocol C consisted of 62 volumes (64 slices, 128×128 pixels, slice thickness 2.5 mm, pixel size $2.5 \text{ mm} \times 2.5 \text{ mm}$), representing 60 GD ($b = 1000 \text{ s/mm}^2$) and two scans with $b = 0$; TE and TR were 28 ms and 3080 ms.

2.3. Data analysis

The postprocessing and statistical analysis (Fig. 1) was performed by use of the analysis software *Tensor Imaging and Fiber Tracking* (TIFT – Müller et al., 2007a).

2.3.1. DTI data analysis

In order to spatially normalize the data to the Montreal Neurological Institute (MNI) stereotaxic space, study-specific templates were created and MNI normalization was performed iteratively (Müller et al., 2016). From the stereotaxically normalized DTI data sets, FA maps were calculated for quantitative mapping of microstructure (Le Bihan et al., 2001). In a consecutive step, an 8 mm full width at half maximum Gaussian filter was applied for smoothing of FA maps in order to achieve

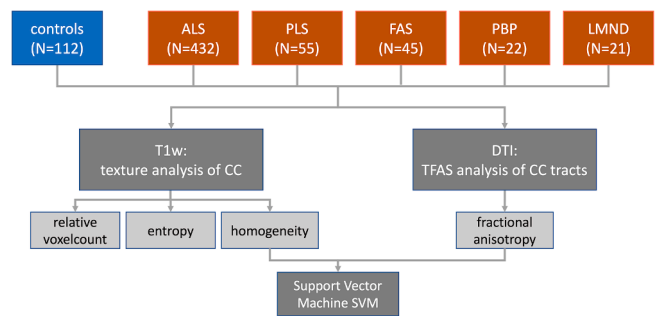


Fig. 1. Analysis scheme. Multiparametric MRI of 575 motor neuron disease (MND) patients with classical amyotrophic lateral sclerosis (ALS) ($N = 432$) or its variants (restricted phenotypes primary lateral sclerosis (PLS) $N = 55$, flail arm syndrome (FAS) $N = 45$, progressive bulbar palsy (PBP) $N = 22$, lower motor neuron disease (LMND) $N = 21$), and 112 healthy controls were analysed for texture parameters in sagittal T1w data and for tract-based fractional anisotropy statistics (TFAS) in callosal tracts of areas I-V, identified from DTI data. In order to further specify the callosal alterations based on textural and diffusion parameters, a support vector machine (SVM) was applied to separate MND patients from controls.

a good balance between sensitivity and specificity (Unrath et al., 2010). FA maps of all subjects were harmonised for different protocols following (Roskopf et al., 2015; Müller et al., 2016; Kalra et al., 2020) and corrected for age (Behler et al., 2021). A correction for gender was not performed as no significant association to gender could be observed in the age-corrected FA maps. From MNI normalized data of controls, an averaged data set was calculated; this data set was used for fibre tracking. To this end, a conventional streamline tracking was used with a vector product threshold of 0.9 (Unrath et al., 2010) and an FA threshold of 0.2 (Müller et al., 2007b) to perform a tract-of-interest (TOI) analysis. The CC could be subdivided into five areas (Hofer and Frahm, 2006): area I tracts are callosal fibres comprising bundles projecting into the prefrontal lobe, area II tracts are callosal fibres projecting to frontal areas including premotor and supplementary motor cortices, area III fibres project to the primary motor cortices, area IV fibres project to primary sensory cortices, and area V fibres project to parietal lobe, occipital lobe, and temporal lobe. Defined tracts originating in CC areas I to V according to this scheme were identified with the TOI approach; the seed placement has been performed in callosal areas I-V with fibre tracking (FT) seed points restricted to the corpus callosum (Müller et al., 2021).

In order to evaluate what the CC may add in comparison with the CST as an established neuroimaging parameter in MND (e.g. Verstraete et al. 2010; Müller et al., 2016), the CST was studied by TOI analysis.

That way, common FT masks could be applied to the individual FA maps. Tract-wise fractional anisotropy statistics (TFAS) (Müller et al., 2007b) was performed by statistically comparing the FA values in each tract between the two groups (Student's *t*-test).

2.3.2. Texture analysis

The previously published analysis cascade (Müller et al., 2020; Bârlescu et al., 2021) contained the following steps: after affine alignment to the anterior commissure/posterior commissure line, the CC was automatically segmented based on an intensity threshold. Then, a subdivision of the CC into areas I–V according to the Hofer and Frahm scheme (Hofer & Frahm, 2006) was performed and finally, calculation of area sizes and texture parameters (Stockman and Shapiro, 2001) was applied.

In the current study, the parameters relative voxel count, entropy, and homogeneity were analyzed. The relative voxel count was calculated by dividing a single area's voxel count through the entire CC's voxel count to detect only focal atrophy of the CC.

The entropy in a given sample increases when the distribution of

intensity values in the sample shows a more inhomogeneous pattern, while the parameter homogeneity rises when grey level differences between neighboring voxels increase (which means that in fact, the structural inhomogeneity rises). Therefore, in the following, we will use the term inhomogeneity for alterations of the tissue property described by the parameter homogeneity. That way, texture parameters could be candidates to identify focal microstructural alterations which are not seen as atrophy. Entropy and homogeneity were chosen as candidate texture parameters, since these parameters had performed best in a previous study on discrimination of callosal texture in neurodegenerative motor neuron disorders and controls (Müller et al., 2020). Therefore, further first- and second-order features (like skewness, kurtosis, correlation, and energy) were not analyzed in the current study.

2.4. Statistical comparison at the group level

All subject groups showed a Gaussian distribution of parameters, and Student's *t*-test was used for comparison at the group level (software: Python 3.9.7). All the results for the comparisons for the five callosal areas were corrected for multiple comparisons (Bonferroni-corrected). To provide a measure of the discriminative power of the combined score, receiver operating characteristic (ROC) curves with area under the curve (AUC) as evaluation parameter for separation quality were calculated; the Youden Index was calculated for each callosal area and each ALS phenotype when compared to controls.

2.5. Support vector machine to discriminate between subject groups

Machine learning (ML) models and large data sets offer unprecedented opportunities for patient stratification and the development of diagnostic, monitoring, and prognostic markers (Grollemund et al., 2019). In this study, in order to separate subject groups, a conventional support vector machine (SVM) (Steinwart and Christmann, 2008) was set up with the following parameters: homogeneity in areas I, II, and III and FA in tracts of callosal areas I, II, and III. In our study group, there was an imbalance between controls and MND patients numbers.

Therefore, the training data set was composed of randomly selected 56 controls (half of the total number of controls), supplemented by (randomly selected) 112 ALS patients (twice the number of controls, no subtypes), and the validation data set, thus, consisted of 463 ALS patients (including subtypes) and 56 controls.

3. Results

3.1. Relative voxel count of the areas I – V of the CC

In patients with PLS, the CC showed a significantly reduced relative voxel count (which is interpreted as callosal atrophy) in area III, while in patients with classical ALS and all other phenotypes, no significant alterations of CC areas I – V could be detected at the group level when compared to controls, including non-significant results for callosal area III at group level although it appeared atrophied in some individual patients by visual inspection, as previously described (Kassubek et al., 2012). In summary, these results indicated that focal atrophy of the CC seems to be a relevant neuroimaging feature only for PLS (Fig. 2). No significant association of area III size with disease duration or ALS-FRS-R was observed.

3.2. Alterations of texture of the CC

The texture parameters for patients with the different ALS phenotypes at the group level are summarized in Fig. 2; the results for patient groups are presented as differences to the mean values of controls. All ALS phenotypes presented increased entropy and increased inhomogeneity in CC areas I, II, and III compared to controls, while areas IV and V showed no significant differences. Most prominent differences were observed in areas II and III. There was no association of texture parameters with disease duration or ALS-FRS-R in callosal areas.

3.3. Tract-based FA results

The TOI analysis showed TFAS results for ALS phenotypes at the

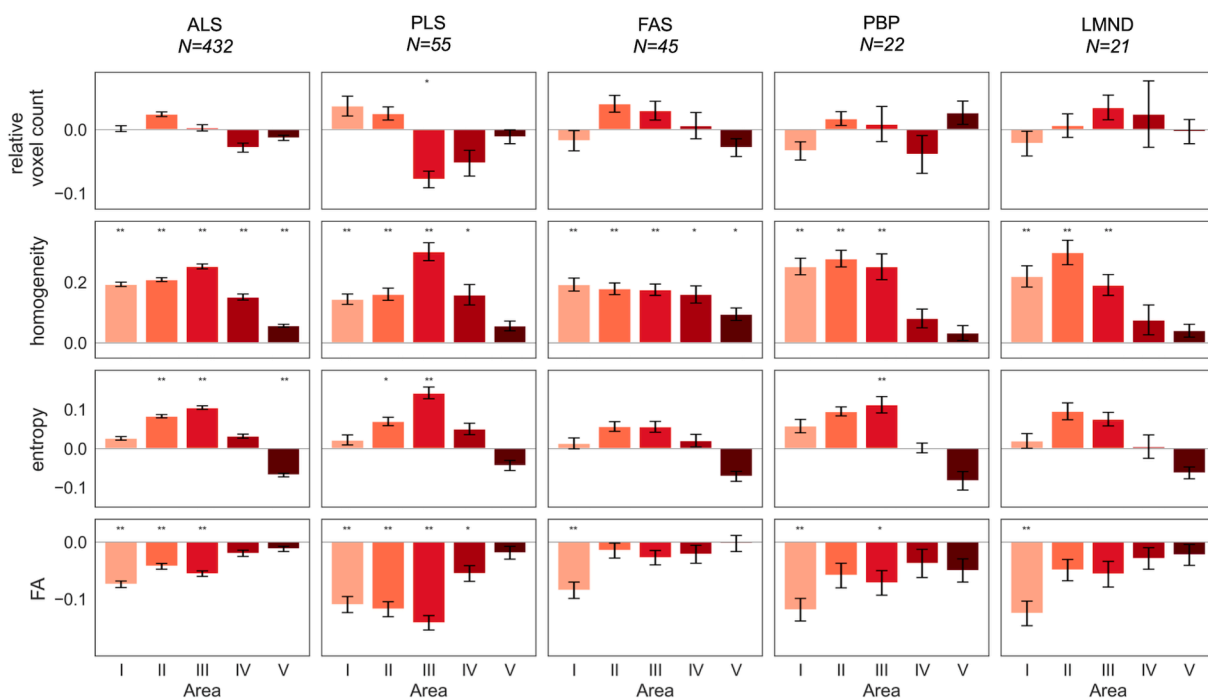


Fig. 2. Relative difference to healthy controls at the group level of relative voxel count, texture parameters (homogeneity and entropy) in callosal areas I-V, and fractional anisotropy (FA) in callosal tracts for amyotrophic lateral sclerosis (ALS) patients and phenotypes (restricted phenotypes primary lateral sclerosis (PLS), flail arm syndrome (FAS), progressive bulbar palsy (PBP), lower motor neuron disease (LMND)). * *p* < 0.01; ** *p* < 0.0001, corrected for multiple comparisons.

group level which are summarized in Fig. 2. All ALS phenotypes, except from FAS, presented with decreased FA in CC areas I, II, and III compared to controls, while areas IV and V showed no differences. Most prominent differences were observed in areas II and III for ALS and PLS. There was no significant association of texture parameters with disease duration or ALS-FRS-R in callosal areas.

3.4. Receiver operating characteristic curves for homogeneity and FA

The relative distribution of the texture parameter homogeneity in callosal areas I – V (homogeneity is preferred compared to entropy in the following analysis as homogeneity shows higher differences between

MND and controls compared to entropy – Fig. 2) and DTI parameter FA of tracts from callosal areas I – V for MND patients compared to controls is shown in Fig. 3. The best separation (lowest overlap) was received for callosal area III, followed by moderate separation in callosal areas I and II, while almost no separation (high overlap) was observed in callosal areas IV and V. Fig. 4 shows the corresponding ROC curves. When averaged for all five ALS phenotypes (without weighting for patient numbers) and averaged for homogeneity and FA, the AUC values are ‘excellent’, i.e., area I, 0.84; area II, 0.81; area III, 0.82 (Mandrekar, 2010). Highest AUC values were found for CC area III; lowest AUC values were found for CC areas IV and V. Fig. 5 shows the Youden Index (homogeneity and FA) for all callosal areas for all ALS phenotypes.

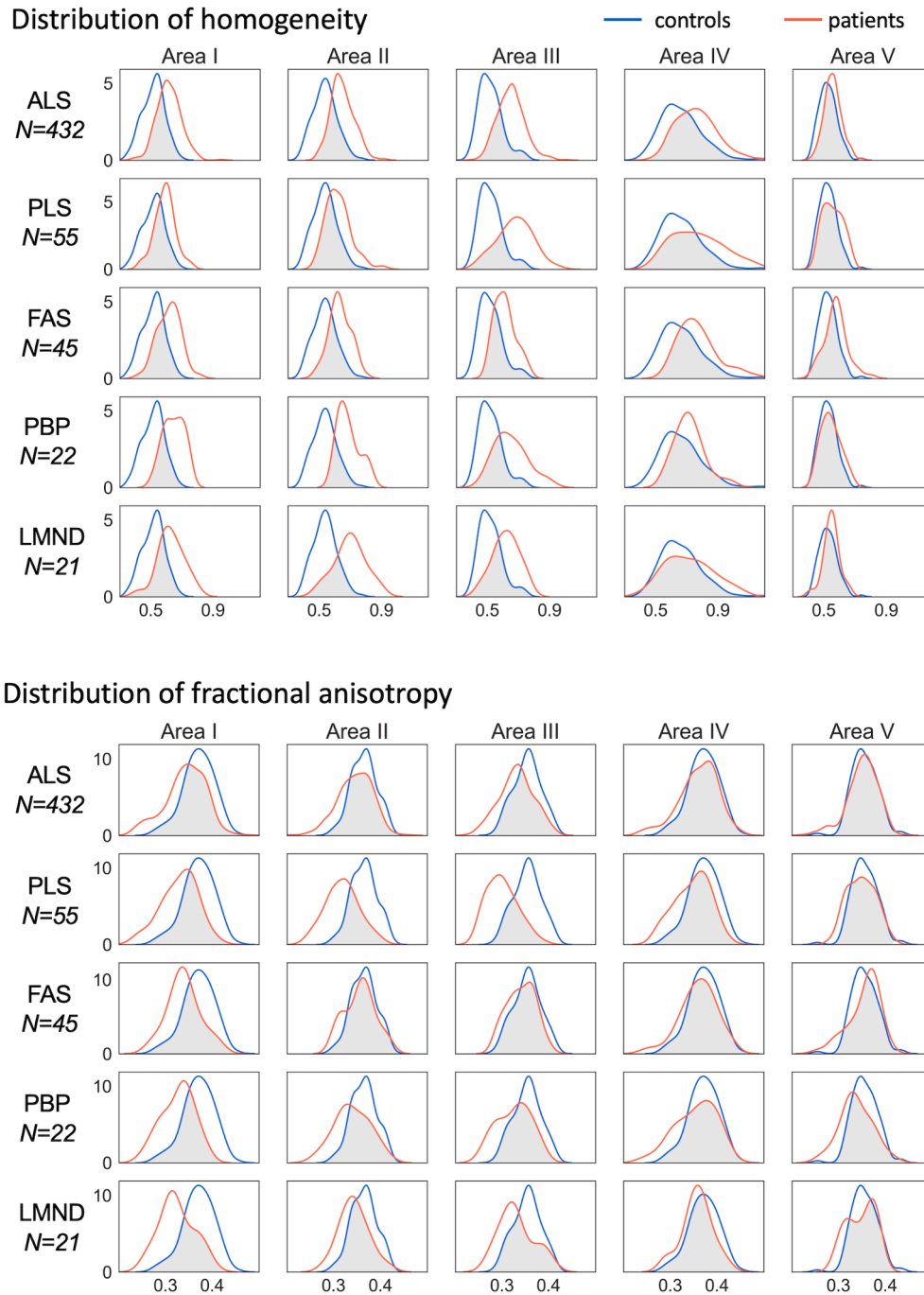
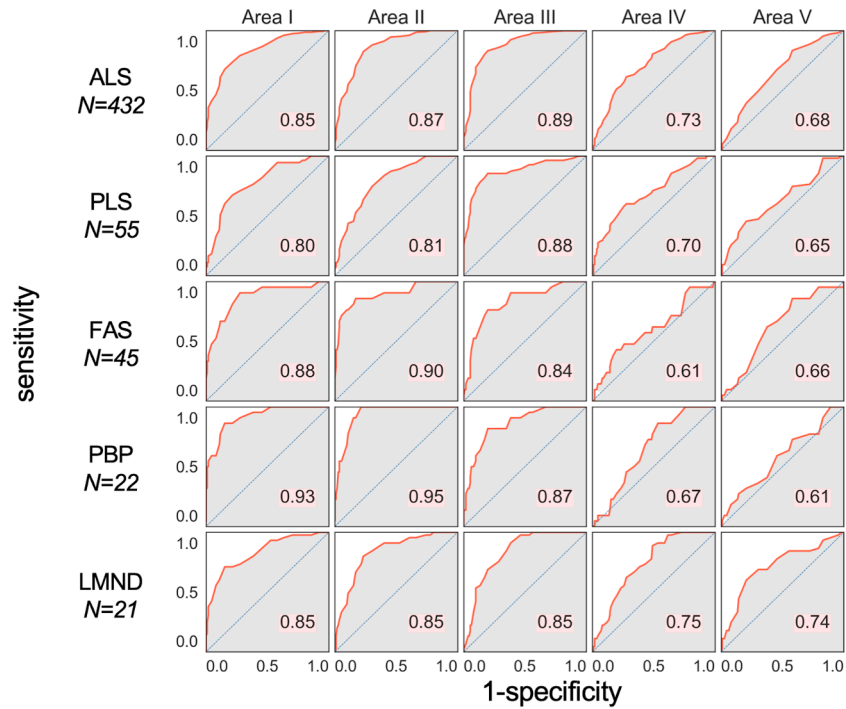


Fig. 3. Distribution of homogeneity (upper panel) and fractional anisotropy (lower panel) in callosal areas I – V for classical amyotrophic lateral sclerosis (ALS) and its phenotypes (restricted phenotypes primary lateral sclerosis (PLS), flail arm syndrome (FAS), progressive bulbar palsy (PBP), lower motor neuron disease (LMND)) (red) compared to controls (blue). The overlap of distributions is shaded in grey. A small overlap represents a good separation of both groups.

ROC curves of homogeneity



ROC curves of fractional anisotropy

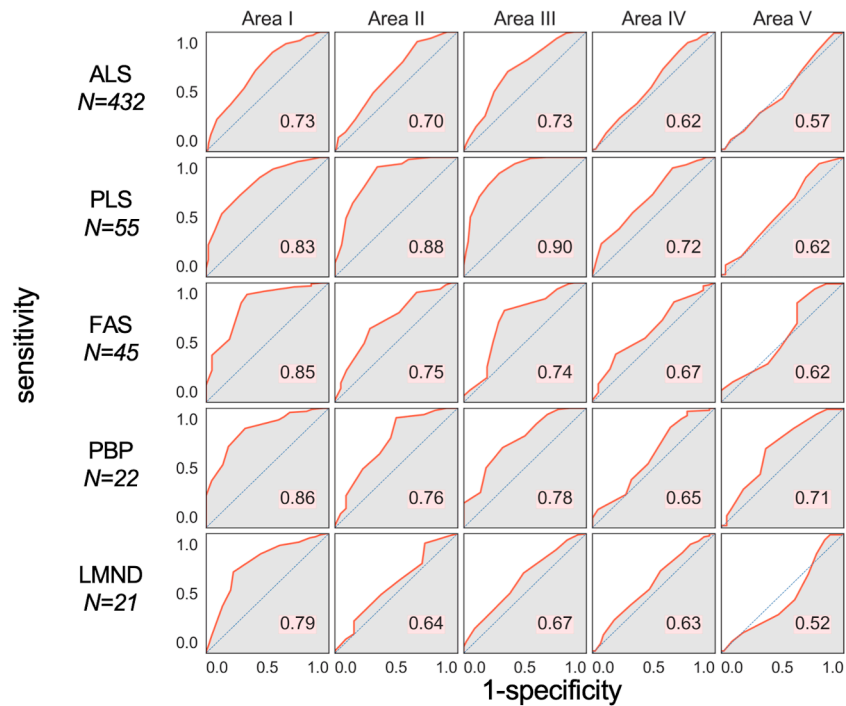


Fig. 4. Receiver operating characteristic (ROC) curves of homogeneity (**upper panel**) and fractional anisotropy (**lower panel**) in callosal areas I-V for amyotrophic lateral sclerosis (ALS) and phenotypes (restricted phenotypes primary lateral sclerosis (PLS), flail arm syndrome (FAS), progressive bulbar palsy (PBP), lower motor neuron disease (LMND)).

3.5. Results for the CST

Fig. 6A shows the relative differences of FA values along the CST for the separate MND groups versus controls and the corresponding ROC curves. Separation of all patients with MND from controls revealed a sensitivity of 78% and a specificity of 59% (Fig. 6B); this results in an

AUC value of 0.75 which is in the range of previous studies (Kassubek et al., 2014).Fig. 7..

3.6. Support vector machine analysis

An SVM was applied in order to discriminate MND patients from

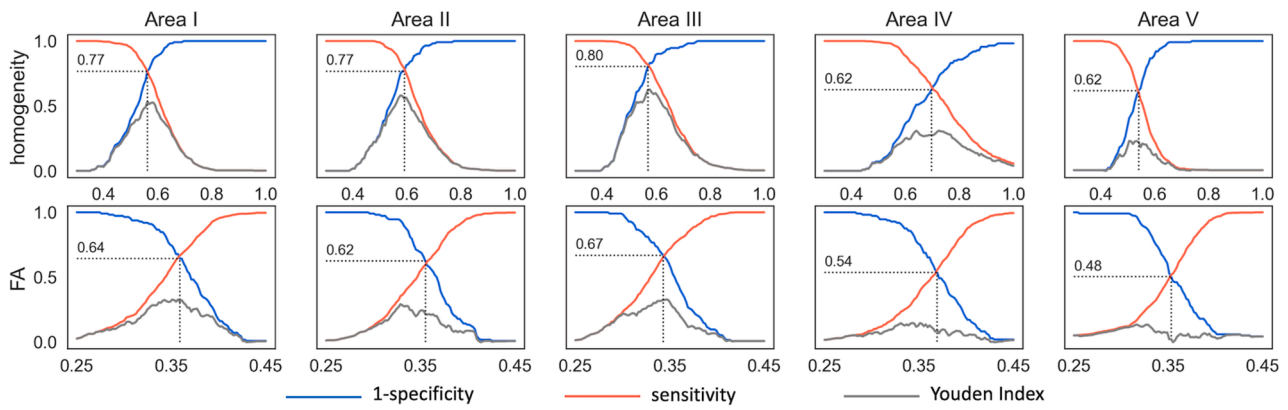


Fig. 5. Youden Index (grey), sensitivity (red) and (1-specificity) (blue) in callosal areas I-V for homogeneity (**upper panel**) and fractional anisotropy (FA) (**lower panel**) for the separation of all patients with motor neuron disease (MND) from controls.

Tractwise FA analysis in the CST

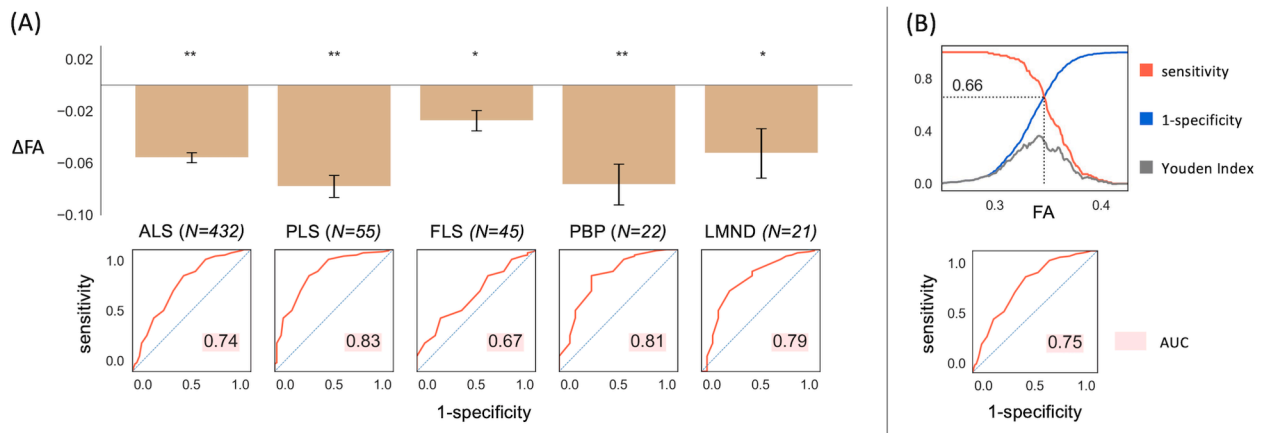


Fig. 6. (A) Relative difference of fractional anisotropy (FA) to healthy controls in the corticospinal tract (CST) at the group level (upper panel) and receiver operating characteristic (ROC) curves (lower panel) for amyotrophic lateral sclerosis (ALS) patients and the restricted phenotypes primary lateral sclerosis (PLS), flail arm syndrome (FAS), progressive bulbar palsy (PBP), lower motor neuron disease (LMND). * $p < 0.01$; ** $p < 0.0001$, corrected for multiple comparisons. **(B)** Youden Index (grey), sensitivity (red) and (1-specificity) (blue) for fractional anisotropy (FA) in the CST for the separation of all patients with motor neuron disease (MND) from controls. The receiver operating characteristic (ROC) curve reveals an area under curve (AUC) value which is interpreted as „acceptable“.

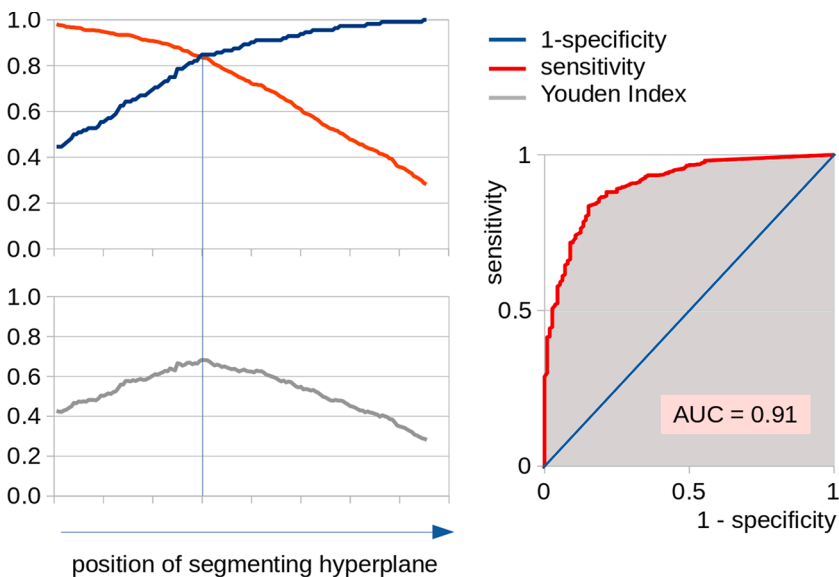


Fig. 7. Left panel: Sensitivity, (1-specificity), and Youden Index for different positions of the segmenting hyperplane for the separation of patients with motor neuron disease (MND) from controls by a six parameter support vector machine (SVM) including homogeneity for plane texture analysis of the corpus callosum (CC) areas I, II, and III, and the fractional anisotropy (FA) of the fibre tracts of these areas – the vertical line is indicating optimum separation, i.e., the minimum difference between sensitivity and specificity. **Right panel:** Receiver operating characteristic (ROC) curve. The area under curve (AUC) value is interpreted as ‘outstanding’.

controls by using the parameters homogeneity in areas I, II, and III and FA in tracts of callosal area I, II, and III. By variation of the position of the segmenting hyperplane (parallel shift), optimum separation was defined as the minimum difference between sensitivity and (1-specificity); this position also reflects the maximum of the Youden index (Fig. 6, left panel). That way, the application of the SVM yielded a sensitivity of 84% and a specificity of 85% in separating all 575 MND patients from 112 controls. Within the training sample, the SVM achieved 80% sensitivity and 84% specificity; in the validation sample, the SVM achieved 84% sensitivity and 86% specificity (Table 2). The corresponding ROC curve for separating patients with MND from controls by the six parameter SVM revealed an AUC value of 0.91 (Fig. 6, right panel) which is interpreted as ‘outstanding’ (Mandrekar, 2010).

The application of the SVM to ALS phenotypes as validation samples showed sensitivities between 80% (FAS) and the highest value of 87% (PLS) for the identical training sample consisting of 112 ALS and 56 controls (Table 2).

When focusing the analysis on two area III parameters, i.e., homogeneity in area III and FA in tracts of callosal area III, the SVM achieved 72% sensitivity and 73% specificity; the three FA parameters in tracts of callosal areas I, II, and III reached a sensitivity of 65% and a specificity of 67% (Table 2).

4. Discussion

The aim of this study was to investigate the segmental microstructural CC morphology in a large cohort of ALS patients including different clinical phenotypes by an MRI parameter combination. To this end, this multiparametric MRI study combined a T1w MRI texture analysis of the CC segments (2D in-plane parameter calculation) and a DTI-based TOI analysis of the corresponding callosal tracts (3D tract-wise analysis); the

Table 2

Results of the support vector machine (SVM) analysis. FA – fractional anisotropy; ALS – amyotrophic lateral sclerosis; MND – motor neuron disease; PLS – primary lateral sclerosis; FAS – flail arm syndrome; PBP – progressive bulbar palsy; LMND – lower motor neuron disease.

	sensitivity / %	specificity / %	Youden Index / %
2 parameters (area III) – FA, homogeneity			
training (112 ALS, 56 controls)	63	82	45
validation (463 MND, 56 controls)	74	64	38
all data (575 MND, 112 controls)	72	73	45
3 parameters (FA area I - III)			
training (112 ALS, 56 controls)	56	70	26
validation (463 MND, 56 controls)	68	64	32
all data (575 MND, 112 controls)	65	67	32
6 parameters (areas I, II, III) FA, homogeneity			
training (112 ALS, 56 controls)	80	84	64
validation (463 MND, 56 controls)	84	86	70
validation (320 ALS, 56 controls)	84	86	70
validation (55 PLS, 56 controls)	87	86	73
validation (45 FAS, 56 controls)	80	86	66
validation (22 PBP, 56 controls)	86	86	72
validation (21 LMND, 56 controls)	86	86	72
all data (575 MND, 112 controls)	84	85	69

DTI approach specifically addressed the callosal fibres which fan out into the white matter of both hemispheres, i.e., the radiation of the CC. The analysis of white matter tract integrity (TFAS) predominantly revealed FA reductions for tracts of the callosal areas I, II, and III for all phenotypes when compared to controls. The texture analysis also demonstrated significant alterations of the parameters entropy and homogeneity in patients with MND for the CC areas I, II, and III compared to controls. An SVM-based analysis of six callosal parameters could achieve a separation of all MND patients (ALS patients including phenotypes) from controls with 84% sensitivity and 85% specificity. This is, with respect to an AUC value of 0.91, an excellent result according to predefined criteria (Mandrekar, 2010) in comparison to other applications of multiparametric MRI classifiers to ALS (review in Thome et al., 2022) and supports the use of CC as a neuroimaging marker in ALS. A recent study (Bede et al., 2022A) used a perceptron model to discriminate ALS, UMN predominant, and LMN predominant cohorts and found that measures of the forceps minor (anterior CC / fibres of the genu of CC) discriminate these subtypes rather well, in the same line like the results of the current study; approaches of neural network classification based on neuroimaging features have also been reported (Bede et al., 2022B).

For the discrimination of classical ALS from controls, the training and validation sample revealed similar results and, moreover, also the validation process for ALS phenotypes showed discrimination results in the same range, indicating that the SVM which was trained for classical ALS also works for ALS phenotypes, with best performance for PLS patients.

This study was focused on the CC in order to investigate the hypothesized biomarker potential of this structure for MND. This multiparametric approach was contrasted to an analysis of the FA values in the CST which is known to be an established neuroimaging parameter in MND (Verstraete et al. 2010; Müller et al., 2016); single parameter analyses of homogeneity in callosal area III, FA in tracts of callosal area III (Fig. 5), and FA in the CST (Fig. 6B) showed all a good performance in discriminating MND patients from controls, i.e. “acceptable” to “excellent” according to Mandrakar (Mandrakar, 2010). However, due to the multiparametric character of the CC-based SVM-analysis, a direct comparison with the monoparametric CST-based analysis in discriminating MND patients from controls cannot be performed.

Beside FA, further DTI metrics like axial diffusivity, radial diffusivity, and mean diffusivity have been reported to provide contributions to this field of research (Agosta et al., 2010; Menke et al., 2017; Rosenbohm et al., 2022). However, these parameters together with FA are a parameterization (parameter reduction) of the six components of the diffusion tensor and, thus, are based on the identical original parameter set (Eigenvalues of the diffusion tensor). Thus, if the study focus is not put on specific properties like discrimination between axonal loss and dysmyelination (e.g. Song et al., 2002), these DTI parameters may contain redundant information. FA has shown to be the most robust DTI metric to demonstrate pathological structural connectivity patterns in MND and to discriminate MND patients from controls (e.g. Verstraete et al., 2010; Müller et al., 2016).

Regional (segmental) alterations of texture and FA in CC areas I, II, and III, thus, seem to constitute a common MRI feature of all investigated phenotypes of ALS. Our study could demonstrate its segmentwise changes in association with ALS with a pathotopography including the central part as the maximum and the two frontal segments to a substantial but lesser extent, while the two posterior parts were not affected, supporting the CC segment V as a structure which is not affected by ALS pathology and can be used as a reference area in FA-based neuroimaging studies in ALS (Kassubek et al., 2018). In the combination of texture analysis and tract-based analysis, the highest alterations for ALS were observed in the CC area III, demonstrating that the maximum of alterations was localized in this segment. The focus on segment III is in line with various advanced neuroimaging studies in ALS, including a voxel-based meta-analysis of DTI datasets from a total of 14 studies which

resulted in one of the peak clusters in the CC body (Zhang et al., 2018) and a fixel-based DTI analysis which demonstrated reduced fibre density and morphology in the motor segments of the CC (Ogura et al., 2022). In agreement with our data which demonstrated the strongest effects of segment III alterations in the PLS subgroup (which was, in addition, the only subgroup with a macrostructural atrophy of segment III with respect to relative voxel count), the motor segment involvement was regarded as a correlate predominantly of the UMN involvement (Zhang et al., 2018). In another study, the approach of mean apparent propagator MRI for diffusion-weighted imaging was applied to a group of 52 ALS patients and demonstrated alterations in the middle and the anterior parts of the CC, corresponding to segments III and II, in a line of agreement with our findings (Chen et al., 2021). With respect to DTI analysis, the identification of the signature of FA decrease relative to healthy controls in the motor callosal fibres in ‘classical’ ALS was also consistent with a previous study by Spinelli and colleagues (Spinelli et al., 2020) who argued that WM microstructural rearrangements occur early in ALS disease course and that once WM degeneration of the callosal fibres has started, this tends towards a greater rate of deterioration (Spinelli et al., 2020). Additionally, by use of a fixel-based analytical method, patients with ALS showed decreased fibre density values (assessing WM microstructural changes), as well as decreased fibre-bundle cross-section (assessing WM macrostructural changes) and decreased fibre density and cross-section values (assessing both microstructural and macrostructural changes) in the middle posterior body of the CC as compared with healthy controls (Cheng et al., 2020). Our approach, however, combined the DTI data with texture measures derived from structural T1w MRI by a SVM and could, thus, substantially increase the discrimination sensitivity and specificity of MND patients and controls.

The study was not without limitations. Although the number of subjects with ALS was high, in fact, one of the largest single-centre MRI studies in MND in the literature to date, the ML models were trained with a comparatively low number of control subjects. This sample size hampered our model’s performance in two respects, first by the limited data quantity of controls compared to MND patients and second by class imbalance. In addition, age differed between the (rather small) group of PBP patients and the other subject groups; however, data analysis included age correction in order to compensate for this difference. Furthermore, some of the restricted phenotype subgroups were of limited sizes which is well explained by the rare occurrence of these clinical presentations; these need to be confirmed in larger (multi-site) cohorts. For the same reason, a gender match of all groups could not be achieved. Disease duration of the PLS group was higher compared to the other groups. Decrease rates (slopes) of ALSFRS-R were higher in PBP and lower in PLS, as it could be expected from the clinical diagnosis. A quantitative score of UMN burden was not included in the analysis. The cross-sectional design allows only assumptions on the time course of changes and provides a basis for the initiation of future longitudinal studies with ALS patients in earlier clinical disease stages.

In conclusion, the combined score encompassing FA and homogeneity for the CC might be included as a candidate for a neuroimaging marker in ALS including the investigated clinical phenotypes. Specifically for the CC segment III, the SVM indicated high potential to discriminate between MND and controls, while it has to be considered that the inclusion of parameters of callosal areas I and II further increases the discrimination power. This unbiased multiparametric MRI approach might, thus, be considered to be an element of future artificial intelligence-guided multimodal models encompassing combinations of multiple clinical and imaging biomarkers for ALS biomarker development (Grollemund et al., 2019).

5. Statement

All human studies have been approved by the appropriate ethics committee and have therefore been performed in accordance with the

ethical standards laid down in the 1964 Declaration of Helsinki and its later amendments.

Funding

This study was supported by the German Research Foundation (Deutsche Forschungsgemeinschaft, DFG Grant Number LU 336/15–1) and the German Network for Motor Neuron Diseases (BMBF 01GM1103A).

CRedit authorship contribution statement

Maximilian Münch: Formal analysis, Investigation, Visualization, Writing – original draft. **Hans-Peter Müller:** Conceptualization, Formal analysis, Investigation, Methodology, Software, Supervision, Writing – original draft. **Anna Behler:** Data curation, Formal analysis, Writing – review & editing. **Albert C. Ludolph:** Investigation, Funding acquisition, Writing – review & editing. **Jan Kassubek:** Project administration, Conceptualization, Supervision, Investigation, Writing – original draft.

Declaration of Competing Interest

The authors declare that they have no known competing financial interests or personal relationships that could have appeared to influence the work reported in this paper.

Acknowledgements

Sonja Fuchs is thankfully acknowledged for her great help in the acquisition of MRI data. The authors would like to thank the Ulm University Center for Translational Imaging MoMAN for its support.

References

- Agosta, F., Galantucci, S., Riva, N., Chiò, A., Messina, S., Iannaccone, S., Calvo, A., Silani, V., Copetti, M., Falini, A., Comi, G., Filippi, M., 2014. Intra-hemispheric and inter-hemispheric structural network abnormalities in PLS and ALS. *Hum. Brain Mapp.* 35, 1710–1722.
- Agosta, F., Pagani, E., Petrolini, M., Caputo, D., Perini, M., Prella, A., Salvi, F., Filippi, M., 2010. Assessment of white matter tract damage in patients with amyotrophic lateral sclerosis: a diffusion tensor MR imaging tractography study. *AJNR Am. J. Neuroradiol.* 31, 1457–1461.
- Agosta, F., Spinelli, E.G., Filippi, M., 2018. Neuroimaging in amyotrophic lateral sclerosis: current and emerging uses. *Expert Rev. Neurother.* 18, 395–406.
- Bârlescu, L.A., Müller, H.P., Uttner, I., Ludolph, A.C., Pankhardt, E.H., Huppertz, H.J., Kassubek, J., 2021. Segmental alterations of the corpus callosum in progressive supranuclear palsy: A multiparametric magnetic resonance imaging study. *Front. Aging Neurosci.* 13, 720634.
- Bede, P., Omer, T., Finegan, E., Chipika, R.H., Iyer, P.M., Doherty, M.A., Vajda, A., Pender, N., McLaughlin, R.L., Hutchinson, S., Hardiman, O., 2018. Connectivity-based characterisation of subcortical grey matter pathology in frontotemporal dementia and ALS: a multimodal neuroimaging study. *Brain Imaging Behav.* 12, 1696–1707.
- Bede, P., Siah, W.F., McKenna, M.C., Shing, L.H., S., 2020. Consideration of C9orf72-associated ALS-FTD as a neurodevelopmental disorder: insights from neuroimaging. *J. Neurol. Neurosurg. Psychiatry* 91, 1138.
- Bede, P., Murad, A., Lope, J., Li Hi Shing, S., Finegan, E., Chipika, R.H., Hardiman, O., Chang, K.M., 2022a. Phenotypic categorisation of individual subjects with motor neuron disease based on radiological disease burden patterns: A machine-learning approach. *J. Neurol. Sci.* 432, 120079.
- Bede, P., Murad, A., Hardiman, O., 2022b. Pathological neural networks and artificial neural networks in ALS: diagnostic classification based on pathognomonic neuroimaging features. *J. Neurol.* 269 (5), 2440–2452.
- Behler, A., Kassubek, J., Müller, H.P., 2021. Age-related alterations in DTI metrics in the human brain—consequences for age correction. *Front. Aging Neurosci.* 13, 682109.
- Brooks, B.R., Miller, R.G., Swash, M., Munsat, T.L., 2000. El Escorial revisited: Revised criteria for the diagnosis of amyotrophic lateral sclerosis. *Amyotroph Lateral Scler Other Motor Neuron Disord.* 1, 293–299.
- Cardenas, A.M., Sarlls, J.E., Kwan, J.Y., Bageac, D., Gala, Z.S., Danielian, L.E., Ray-Chaudhury, A., Wang, H.W., Miller, K.L., Foxley, S., Jbaldi, S., Welsh, R.C., Floeter, M.K., 2017. Pathology of callosal damage in ALS: an ex-vivo, 7 T diffusion tensor MRI study. *NeuroImage Clin.* 15, 200–208.
- Cedarbaum, J.M., Stambler, N., Malta, E., Fuller, C., Hilt, D., Thurmond, B., Nakanishi, A., 1999. The ALSFRS-R: a revised ALS functional rating scale that incorporates assessments of respiratory function. BDNF ALS study group (phase III). *J. Neurol. Sci.* 169, 13–21.

- Chapman, M.C., Jelsone-Swain, L., Johnson, T.D., Gruis, K.L., Welsh, R.C., 2014. Diffusion tensor MRI of the corpus callosum in amyotrophic lateral sclerosis. *J. Magn. Reson. Imaging* 39, 641–647.
- Chen, H.J., Zhan, C., Cai, L.M., Lin, J.H., Zhou, M.X., Zou, Z.Y., Yao, X.F., Lin, Y.J. 2021. White matter microstructural impairments in amyotrophic lateral sclerosis: A mean apparent propagator MRI study. *Neuroimage Clin.* 32, 102863.
- Cheng, L., Tang, X., Luo, C., Liu, D., Zhang, Y., Zhang, J., 2020. Fiber-specific white matter reductions in amyotrophic lateral sclerosis. *Neuroimage Clin.* 28, 102516.
- Chiò, A., Calvo, A., Moglia, C., Mazzini, L., Mora, G., PARALS study group., 2011. Phenotypic heterogeneity of amyotrophic lateral sclerosis: a population based study. *J. Neurol. Neurosurg. Psychiatry* 82, 740–746.
- Chiò, A., Pagani, M., Agosta, F., Calvo, A., Cistaro, A., Filippi, M., 2014. Neuroimaging in amyotrophic lateral sclerosis: insights into structural and functional changes. *Lancet Neurol.* 13, 1228–1240.
- de Vries, B.S., Rustemeijer, L.M.M., Bakker, L.A., Schröder, C.D., Veldink, J.H., van den Berg, L.H., Nijboer, T.C.W., van Es, M.A., 2019. Cognitive and behavioural changes in PLS and PMA: challenging the concept of restricted phenotypes. *J. Neurol. Neurosurg. Psychiatry* 90, 141–147.
- Filippini, N., Douaud, G., Mackay, C.E., Knight, S., Talbot, K., Turner, M.R., 2010. Corpus callosum involvement is a consistent feature of amyotrophic lateral sclerosis. *Neurology.* 75, 1645–1652.
- Filippi, M., Agosta, F., Grosskreutz, J., Benatar, M., Kassubek, J., Verstraete, E., Turner, M.R.; Neuroimaging Society in ALS (NISALS). 2015. Progress towards a neuroimaging biomarker for amyotrophic lateral sclerosis. *Lancet Neurol.* 14, 786–788.
- Foerster, B.R., Welsh, R.C., Feldman, E.L., 2013. 25 years of neuroimaging in amyotrophic lateral sclerosis. *Nat Rev Neurol.* 9, 513–524.
- Finegan, E., Chipika, R.H., Shing, S.L.H., Hardiman, O., Bede, P., 2019. Primary lateral sclerosis: a distinct entity or part of the ALS spectrum? *Amyotroph Lateral Scler. Frontotemporal Degener.* 20, 133–145.
- Grollemund, V., Pradat, P.F., Querin, G., Delbot, F., Le Chat, G., Pradat-Peyre, J.F., Bede, P., 2019. Machine learning in amyotrophic lateral sclerosis: achievements, pitfalls, and future directions. *Front. Neurosci.* 13, 135.
- Hofer, S., Frahm, J., 2006. Topography of the human corpus callosum revisited – comprehensive fiber tractography using diffusion tensor magnetic resonance imaging. *Neuroimage* 32, 989–994.
- Hübbers, A., Hildebrandt, V., Petri, S., Kollwe, K., Hermann, A., Storch, A., Hanisch, F., Zierz, S., Rosenbohm, A., Ludolph, A.C., Dorst, J., 2016. Clinical features and differential diagnosis of flail arm syndrome. *J. Neurol.* 263, 390–395.
- Kalra, S., Müller, H.P., Ishaque, A., Zinman, L., Korngut, L., Genge, A., Beaulieu, C., Frayne, R., Graham, S.J., Kassubek, J., 2020. A prospective harmonized multicenter DTI study of cerebral white matter degeneration in ALS. *Neurology* 95, e943–e952.
- Kassubek, J., Ludolph, A.C., Müller, H.P., 2012. Neuroimaging of motor neuron diseases. *Ther Adv Neurol Disord.* 5, 119–127.
- Kassubek, J., Müller, H.P., Del Tredici, K., Lulé, D., Gorges, M., Braak, H., Ludolph, A.C., 2018. Imaging the pathoanatomy of amyotrophic lateral sclerosis in vivo: targeting a propagation-based biological marker. *J. Neurol. Neurosurg. Psychiatry* 89, 374–381.
- Kassubek, J., Müller, H.P., 2020. Advanced neuroimaging approaches in amyotrophic lateral sclerosis: refining the clinical diagnosis. *Expert Rev. Neurother.* 20, 237–249.
- Kassubek, J., Müller, H.P., Del Tredici, K., Bretschneider, J., Pinkhardt, E.H., Lulé, D., Böhm, S., Braak, H., Ludolph, A.C., 2014. Diffusion tensor imaging analysis of sequential spreading of disease in amyotrophic lateral sclerosis confirms patterns of TDP-43 pathology. *Brain.* 137, 1733–1740.
- Kocar, T.D., Behler, A., Ludolph, A.C., Müller, H.P., Kassubek, J., 2021. Multiparametric microstructural MRI and machine learning classification yields high diagnostic accuracy in amyotrophic lateral sclerosis: proof of concept. *Front. Neurol.* 12, 745475.
- Le Bihan, D., Mangin, J.F., Poupon, C., Clark, C.A., Pappata, S., Molko, N., Chabriat, H., 2001. Diffusion tensor imaging: concepts and applications. *J. Magn. Reson. Imaging* 13, 534–546.
- Ludolph, A., Drory, V., Hardiman, O., Nakano, I., Ravits, J., Robberecht, W., Shefner, J.; WFN Research Group On ALS/MND. 2015. A revision of the El Escorial criteria - 2015. *Amyotroph Lateral Scler. Frontotemporal Degener.* 29, 1–2.
- Mandrekar, J.N., 2010. Receiver operating characteristic curve in diagnostic test assessment. *J Thorac Oncol.* 5, 1315–1316.
- Menke, R.A.L., Proudfoot, M., Talbot, K., Turner, M.R., 2017. The two-year progression of structural and functional cerebral MRI in amyotrophic lateral sclerosis. *Neuroimage Clin.* 17, 953–961.
- Müller, H.P., Lulé, D., Roselli, F., Behler, A., Ludolph, A.C., Kassubek, J. 2021. Segmental involvement of the corpus callosum in C9orf72-associated ALS: a tract of interest-based DTI study. *Ther Adv Chronic Dis.* 12, 20406223211002969.
- Müller, H.P., Turner, M.R., Grosskreutz, J., Abrahams, S., Bede, P., Govind, V., Prudlo, J., Ludolph, A.C., Filippi, M., Kassubek, J.; Neuroimaging Society in ALS (NISALS) DTI Study Group. 2016. A large-scale multicentre cerebral diffusion tensor imaging study in amyotrophic lateral sclerosis. *J Neurol Neurosurg Psychiatry.* 87, 570–579.
- Müller, H.P., Dreyhaupt, J., Roselli, F., Schlecht, M., Ludolph, A.C., Huppertz, H.J., Kassubek, J. 2020. Focal alterations of the callosal area III in primary lateral sclerosis: an MRI planimetry and texture analysis. *Neuroimage Clin.* 26, 102223.
- Müller, H.P., Unrath, A., Ludolph, A.C., Kassubek, J., 2007a. Preservation of diffusion tensor properties during spatial normalisation by use of tensor imaging and fibre tracking on a normal brain database. *Phys. Med. Biol.* 52, N99–N.
- Müller, H.P., Unrath, A., Sperfeld, A.D., Ludolph, A.C., Riecker, A., Kassubek, J., 2007b. Diffusion tensor imaging and tractwise fractional anisotropy statistics: quantitative analysis in white matter pathology. *Biomed. Eng. Online* 6, 42.
- Ogura, A., Kawabata, K., Watanabe, H., Choy, S.W., Bagarinao, E., Kato, T., Imai, K., Masuda, M., Ohdake, R., Hara, K., Nakamura, R., Atsuta, N., Nakamura, T., Katsuno, M., Sobue, G., 2022. Fiber-specific white matter analysis reflects upper motor neuron impairment in amyotrophic lateral sclerosis. *Eur. J. Neurol.* 29, 432–440.
- Rosenbohm, A., Müller, H.-P., Hübbers, A., Ludolph, A.C., Kassubek, J., 2016. Corticoefferent pathways in pure lower motor neuron disease: a diffusion tensor imaging study. *J. Neurol.* 263 (12), 2430–2437.
- Rosenbohm, A., Del Tredici, K., Braak, H., Huppertz, H.-J., Ludolph, A.C., Müller, H.-P., Kassubek, J., 2022. Involvement of cortico-efferent tracts in flail arm syndrome: a tract-of-interest-based DTI study. *J. Neurol.* 269 (5), 2619–2626.
- Roskopf, J., Müller, H.P., Dreyhaupt, J., Gorges, M., Ludolph, A.C., Kassubek, J., 2015. Ex post facto assessment of diffusion tensor imaging metrics from different MRI protocols: preparing for multicentre studies in ALS. *Amyotroph. Lateral Scler. Frontotemporal Degener.* 16, 92–101.
- Song, S.-K., Sun, S.-W., Ramsbottom, M.J., Chang, C., Russell, J., Cross, A.H., 2002. Demyelination revealed through MRI as increased radial (but unchanged axial) diffusion of water. *Neuroimage* 17, 1429–1436.
- Spinelli, E.G., Riva, N., Rancoita, P.M.V., Schito, P., Doretti, A., Poletti, B., Di Serio, C., Silani, V., Filippi, M., Agosta, F., 2020. Structural MRI outcomes and predictors of disease progression in amyotrophic lateral sclerosis. *Neuroimage Clin.* 27, 102315.
- Steinwart, I., Christmann, A., 2008. Support Vector Machines. Springer, New York, p. 602.
- Stockman, G., Shapiro, L.G., 2001. Chapter 7. Computer Vision. Prentice Hall PTR Upper Saddle River, NJ, USA.
- Swinnen, B., Robberecht, W., 2014. The phenotypic variability of amyotrophic lateral sclerosis. *Nat Rev Neurol.* 10, 661–670.
- Thome, J., Steinbach, R., Grosskreutz, J., Durstewitz, D., Koppe, G., 2022. Classification of amyotrophic lateral sclerosis by brain volume, connectivity, and network dynamics. *Hum. Brain Mapp.* 43, 681–699.
- Tu, S., Wang, C., Menke, R.A.L., Talbot, K., Barnett, M., Kiernan, M.C., Turner, M.R., 2020. Regional callosal integrity and bilaterality of limb weakness in amyotrophic lateral sclerosis. *Amyotroph Lateral Scler Frontotemporal Degener.* 21, 396–402.
- Turner, M.R., Verstraete, E., 2015. What does imaging reveal about the pathology of amyotrophic lateral sclerosis? *Curr Neurol Neurosci Rep.* 15, 45.
- Unrath, A., Müller, H.P., Riecker, A., Ludolph, A.C., Sperfeld, A.D., Kassubek, J., 2010. Whole brain-based analysis of regional white matter tract alterations in rare motor neuron diseases by diffusion tensor imaging. *Hum. Brain Mapp.* 31, 1727–1740.
- Van den Berg-Vos, R.M., Visser, J., Franssen, H., de Visser, M., de Jong, J.M.B.V., Kalmijn, S., Wokke, J.H.J., Van den Berg, L.H., 2003. Sporadic lower motor neuron disease with adult onset: classification of subtypes. *Brain.* 126 (5), 1036–1047.
- van Es, M.A., Hardiman, O., Chio, A., Al-Chalabi, A., Pasterkamp, R.J., Veldink, J.H., van den Berg, L.H., 2017. Amyotrophic lateral sclerosis. *Lancet* 390, 2084.
- Verstraete, E., van den Heuvel, M.P., Veldink, J.H., Blanken, N., Mandl, R.C., Hulshoff Pol, H.E., van den Berg, L.H. 2010. Motor network degeneration in amyotrophic lateral sclerosis: a structural and functional connectivity study. *PLoS One.* 5, e13664.
- Wijesekera, L.C., Mathers, S., Talman, P., Galtrey, C., Parkinson, M.H., Ganesalingam, J., Willey, E., Ampong, M.A., Ellis, C.M., Shaw, C.E., Al-Chalabi, A., Leigh, P.N., 2009. Natural history and clinical features of the flail arm and flail leg ALS variants. *Neurology.* 72, 1087–1094.
- Zhang, F., Chen, G., He, M., Dai, J., Shang, H., Gong, Q., Jia, Z., 2018. Altered white matter microarchitecture in amyotrophic lateral sclerosis: A voxel-based meta-analysis of diffusion tensor imaging. *Neuroimage Clin.* 19, 122–129.